

**Military Technical  
College  
Kobry El-Kobbah,  
Cairo, Egypt**



**11th International  
Conference on Electrical  
Engineering  
ICEENG 2018**

## **High Throughput Data Relay Satellite Link at Ka/Q/W Bands for Earth Observation Missions**

S.H.Mohamed\* , B.G.Evans\*\*

### **ABSTRACT**

Captured data by earth observing low earth orbit satellites are downlinked to the gateways at very low data rates limited by the congested X and S bands. A data relay link by a geostationary orbit satellite was proposed to collect the captured data from several low earth orbit satellites from its higher altitude and feeds it to the gateways. A high throughput feeder downlink was achieved by migration to higher and less congested Q and W frequency bands aiming to achieve higher data rates. The achieved data rates by the modelled data relay links at Ka, Q and W bands were very promising in clear sky conditions never the less the satellite channel was an obstacle specifically at Q and W bands, where the satellite link showed a very poor availability and significantly deteriorated capacity. Hence propagation channel models were derived for each band and fade mitigation techniques were investigated and employed. The links at Q and W bands employed site diversity fade mitigation technique being the only possible strategy within the existing technology together with variable code and modulation. Selective, equal gain and maximum gain combining site diversity techniques were modelled and evaluated for three diversity scenarios for all the European earth observation programme gateways. The designed data relay link at Q and W bands achieved the high throughput data demand by Copernicus European Earth observation programme while maintaining the system's ground segment complexity. This solution could be extended to provide a near live streaming service which is limited by the low earth orbit satellites constellation design and number of geostationary orbit satellites.

**Keywords — Satellite Communications , Data Relay Links , High Throughput , Fade mitigation , Earth Observation , Diversity , Link Budget**

---

\* Egyptian Armed Forces

\*\* Comm. Systems Research Centre, University of Surrey, Guildford, United Kingdom.

## I. INTRODUCTION

Typical earth observation system consists of a constellation of sun-synchronous, polar low earth orbit satellites (LEO). Forty LEO satellites provide global coverage offering less downlink transmission power from the satellite to the gateway to close the link budget in comparison with medium earth orbit (MEO) and geostationary earth orbit (GEO) satellites, as well as high frequency reuse efficiency. On the other hand, low earth orbit satellite systems are complex in terms of handovers design and interference management. Also, they require large network of globally spread gateways with restricted configurations due to political regulations. A massive increase in the ground segment's cost and complexity is a one more drawback that confronts the overall system design. Another system structure was investigated which takes full benefit of the typical structure while mitigating its drawbacks. The new structure included a data relay link via a higher altitude geostationary earth orbit (GEO) satellite at which just three satellites can provide global coverage excluding the poles and hence the ground segment complexity reduces significantly. A feeder downlink from the geostationary earth orbit (GEO) satellite then down streams the captured data by the low earth orbit (LEO) satellites in operation to the gateways [1] once they are received at the GEO satellite terminal.

Earth observation missions have been involved in lots of applications such as natural resources survey, climate and disasters monitoring, agriculture, maritime services, surveillance and security. Advanced earth observation satellites are equipped with very high resolution observation systems which capture high resolution images and videos, or even sounds as recorded by the Meteosat third generation satellites at very high data rates in the range of megabytes per second [2]. To employ an efficient feeder downlink from a geostationary earth orbit satellite that collected data from all low earth orbit satellites in operation a very high capacity transmission [1] is demanded or else a very large on board memory for data buffering which is a less efficient solution that would be avoided by spacecraft's manufacturers and more importantly by delay intolerant applications that require online streaming. Consequently, strategies to improve the capacity of the earth observation communication system had been essential [2, 3]. Migration to higher frequency bands such as Q and W bands for feeder downlink was one strategy that had been studied. Challenges regarding these high frequency bands were discussed as well as solutions to overcome these challenges were proposed.

High throughput data relay satellite feeder link design has been of a great interest to earth observation missions. Initially, earth observation missions in operation were to be investigated to have an overview of the current capabilities and demands and develop a wide vision of all possible solutions to improve these capabilities and have an overview of the upcoming challenges. Migration to extreme high frequency bands was confronted by the severe satellite channel especially at Q and W bands where site diversity fade mitigation technique was to be investigated to determine the system's applicability at Q and W bands.

## II. STATE OF THE ART

### A. Earth observation programmes

Landsat 8 had a downlink data rate of 260.92 Mbps in S-band and 384 Mbps in X-band and storage capacity of 3.14 Tb. Landsat 8 was designed to capture 400 images per day, nevertheless it was capable of capturing 725 images per day which was required to increase the probability of cloud free images .

Meteosat third generation will be one of the most recent earth observation programmes in 2018 launched to a Geostationary orbit at an altitude of approximately 35,786 Km. The programme consists of 6 satellites, at which 2 infrared and ultraviolet sounder satellites to deliver temperature and humidity broadcasts as well as storms warning and pollution monitoring applications. The other 4 satellites are high resolution optical imaging satellites with telemetry transmission at a data rate of 165Mbps/s, while the sounder satellites will transmit telemetry at data rate of 260 Mbps both in the Ka-band [2, 4].

More European satellites in orbit are Envisat launched in 2002 which was the world's largest civilian Earth observation satellite and currently replaced by sentinel series, ERS-2, Proba-1, Gravity Field & Steady-State Ocean Circulation Explorer (GOCE) launched in 2009 which monitored sea level change, terrestrial ice dynamics and ocean circulation [5]. European Global Monitoring for Environment and Security (GMES) had developed Copernicus programme which aimed to support environmental, climate, land and marine monitoring, as well as emergency management and security. Sentinel-1 and Sentinel-2 satellites were launched in April 2014 by the European space agency (ESA) [7]. Both satellites had a downlink data rate of 260 Mbps on two X-band frequency carriers and they were capable of providing average compressed data throughput of 2.4 TB per day with an on board capacity storage memory of 1.4 Tb each [7].

Finally, Europe's full coverage system, the European data relay satellite system, which is the most complicated optical communication network which supported near real time data transmission to gateways in Europe. It consists of two geostationary satellites EDRS-A launched in January 2016 and EDRS-C to be launched in 2017, both to relay data from all low earth orbiting satellites via optical intersatellite links to gateways in Redu, Belgium, Harwell, Great Britain, Weilheim, Germany and Matera, Italy via Ka band at a data rate of 1.8 Gbps and throughput of 50 TBytes/day. This successful relay system avoided the time delay introduced by direct systems as one data relay satellite can quadruple the time one low earth satellite can be in contact with its gateway (download duration) [8].

### B. High throughput feederlinks

High throughput satellites is a generation of satellites which can transmit at very high data rates up to 140 Gbps as achieved by Viasat -1 in the Ka band [14]. Ka band is currently congested and migration to higher bands such Q and W bands allowed higher transmission bandwidth as mentioned in [1] where Ka band system had a channel bandwidth of 500 MHz while double channel bandwidth was available for Q and W band systems. More advantages offered by Q and W bands operated systems

are increasing the on board antenna gain and hence smaller size on board antenna same as the system in [1] where the Ka band operated satellite had an antenna diameter of 5.2 m where Q and W band operated satellite had an on board antenna diameter of 2.4m This saved half mass in space which is a very critical issue to satellite manufacturers. High gain is then expected at the receiving gateway antenna which motivated the receiver's portability in case fine pointing was maintained by the tracking system especially at these high frequencies. Finally, higher frequency reuse factor is offered by Q and W bands which motivated the multiple spot beams technology. [10,11,12]. According to a study carried out by [13] it was concluded that an increase in system bandwidth together with transmission power which is a by-product of using higher frequency carriers, had caused a capacity gain 6.6 times larger than an increase in the system's transmission power .

### C. Propagation at Q and W bands

Precipitation is the major source of attenuation in the satellite channel, it increases proportionally with the carrier frequency and hence it is most severe at the W band. Moreover, it increases the receiving antenna's noise temperature which degrades its figure of merit significantly consequently the advantage of small dish antennas is lost as large antennas are needed for reception at higher gain to overcome this degradation unless fade mitigation technique was applied. The Statistical model to evaluate the precipitation loss provided by [14] and evaluated by [15] at the W band

## III. METHODOLOGY

The problem statement of designing high throughput data relay satellite feeder links was previously defined and the demand for this link was shown to exist for the coming earth observation systems generations. In this section the problem was tackled and the detailed methodology followed will be explained in details. Figure 1 shows a typical data relay satellite system where the link colored in purple is the optical intersatellite link from the low earth observing orbit satellite to the Geostationary satellite and the link coloured in red and green is the down feeder link to the gateway which was the main concern of this work.

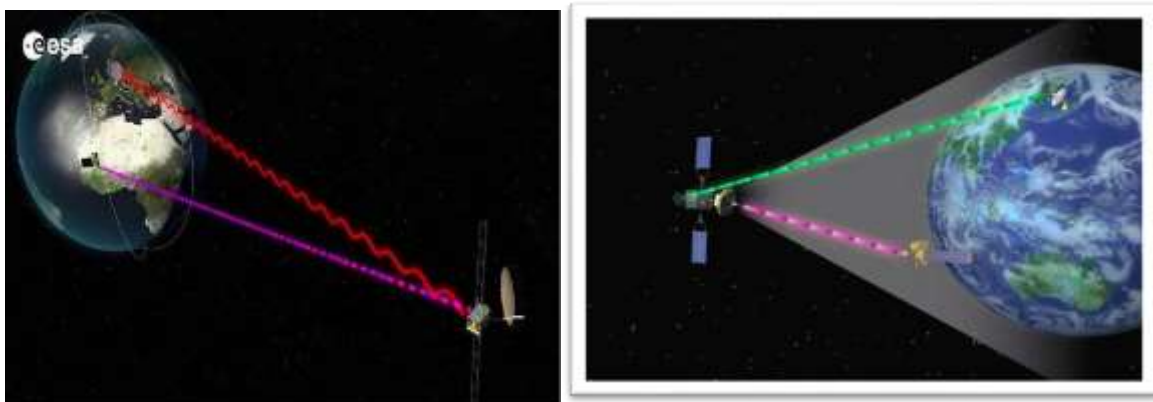


Fig.1. Typical data relay satellite link

The objectives were

- Clear sky link budget analysis at Ka/Q and W bands
- Maximum system capacity evaluation.
- Satellite channel modelling.
- Average capacity evaluation for each of the four gateways of the European earth observation programme Copernicus.
- Link availability evaluation.
- Fade mitigation techniques investigation.
- Site diversity modelling.
- Diversity gain evaluation for different combining techniques and different separation distances for each of the four primary gateways.
- Diversity modelling validation.
- Link's availability and average capacity re-evaluation for each gateway.
- Designed data relay link throughput evaluation at Ka/Q and W bands.

Figure 2 shows the feeder downlink design flow chart in order to fulfil these objectives . Initially the design was obliged to :

- The user's requirements of high data rates up to 6 Gbps.
- Data transfer constraints due to migration to Q & W bands.

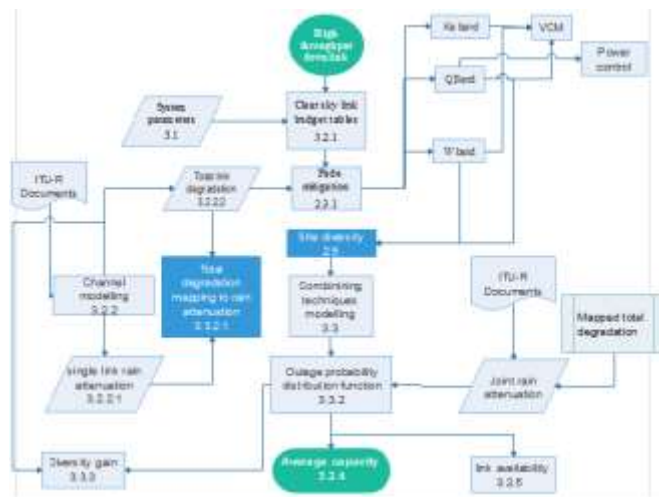


Fig.2. Feeder downlink design flow chart.

First clear sky link budget analysis was performed to evaluate the maximum system capacity, then the propagation channel was modelled using the International Telecommunication Union Recommendations (ITU-R) for rain attenuation .Severe rain and clouds attenuation causes channel fading and hence the average capacity was evaluated under rain conditions. Several fade mitigation techniques were

adopted to mitigate the rain fading and enhance the average capacity and most importantly the link's availability. The adopted fade mitigation techniques were

- Satellite transmitter power control at Q band.
- Variable Code Modulation (VCM) using the CCSDS standard modulation and coding schemes list.
- Site diversity employing three combining techniques which were
  - SELECTRIVE COMBINING (SC)
  - EQUAL GAIN COMBINING (EGC)
  - Maximum Gain Combining (MGC).

The average capacity was re-evaluated when the site diversity fade mitigation technique was employed using the joint rain attenuation distribution as provided by the ITU-R.

#### *A. System Structure*

The system consisted of a geostationary satellite at a longitude of 130° East and 4 primary gateways with locations in Redu, Belgium, Harwell in Great Britain, Weilheim in Germany and Matera in Italy. These gateways are operating for the European data relay satellite system (EDRS) [16]. Table 1 shows the system's structure.

The system was evaluated at Ka, Q and W bands with carrier frequencies of 20GHz, 40 GHz and 74 GHz respectively and hence the gateway system noise temperature and pointing inaccuracy varied with these frequency bands as well as the satellite's amplifier saturation power and channel bandwidths under clear sky conditions. All gateways parameters for all locations were assumed as extracted from [1].

Power control fade mitigation technique was applied to the satellite's transmitter at Q band which justifies power increase of 30 Watts compared to the satellite's transmitter at Ka band, however power control was in applicable to the satellite's transmitter at W band as the amplifier already saturates at 40 W as stated in [1]. A back-off of 5 dB to 1024-APSK modulation scheme with a coding rate of 0.85 was suggested in [1] and applied to avoid the amplifier's non-linear operation. Back-off power for each modulation and coding scheme for the Consultative Committee for Space Data Systems (CCSDS) standard was provided by [1].

To model site diversity for the four primary gateways, three redundant gateways at separation distances of 20Km, 50 Km and 80 Km were selected.

TABLE I. SYSTEM'S STRUCTURE

| Parameter                            | Redu, Belgium           | Harwell England | Weilheim Germany | Matera Italy |
|--------------------------------------|-------------------------|-----------------|------------------|--------------|
| <b>Gateways</b>                      |                         |                 |                  |              |
| Location (degrees)                   | Long                    | Long            | Long             | Long         |
|                                      | 5.16                    | -1.29           | 11.14            | 16.6         |
| Height above mean sea level (m)      | Lat                     | Lat             | Lat              | Lat          |
|                                      | 50                      | 51.6            | 47.84            | 40.67        |
| Antenna diameter (m)                 | 100                     | 100             | 100              | 100          |
| Antenna efficiency(m)                | 9                       | 9               | 9                | 9            |
| Antenna efficiency(m)                | 65                      | 65              | 65               | 65           |
| Noise temperature (K)                | Ka Band                 | Ka Band         | Ka Band          | Ka Band      |
|                                      | 109.46                  | 109.46          | 109.46           | 109.46       |
|                                      | Q Band                  | Q Band          | Q Band           | Q Band       |
|                                      | 122.09                  | 122.09          | 122.09           | 122.09       |
| Gateway pointing inaccuracy (radian) | W Band                  | W Band          | W Band           | W Band       |
|                                      | 177.39                  | 177.39          | 177.39           | 177.39       |
| Gateway pointing inaccuracy (radian) | Ka                      | Ka              | Ka               | Ka           |
|                                      | 0.03                    | 0.03            | 0.03             | 0.03         |
|                                      | Q                       | Q               | Q                | Q            |
|                                      | 0.02                    | 0.02            | 0.02             | 0.02         |
| Gateway pointing inaccuracy (radian) | W                       | W               | W                | W            |
|                                      | 0.02                    | 0.02            | 0.02             | 0.02         |
| <b>Satellite</b>                     |                         |                 |                  |              |
| TWTA saturation (W)                  | Ka 70                   |                 |                  |              |
|                                      | Q 100                   |                 |                  |              |
|                                      | W 40                    |                 |                  |              |
| Transmitter Power (W)                | Ka 65                   |                 |                  |              |
|                                      | Q 95                    |                 |                  |              |
|                                      | W 35                    |                 |                  |              |
| MUX and Waveguide losses (dB)        | 1                       |                 |                  |              |
| Antenna diameter (m)                 | 5.2                     |                 |                  |              |
| <b>Channel</b>                       |                         |                 |                  |              |
| Downlink Frequency (GHz)             | Ka                      | Ka              | Ka               | Ka           |
|                                      | 20                      | 20              | 20               | 20           |
|                                      | Q                       | Q               | Q                | Q            |
|                                      | 40                      | 40              | 40               | 40           |
| Channel bandwidth (MHz)              | W                       | W               | W                | W            |
|                                      | 74                      | 74              | 74               | 74           |
| Channel bandwidth (MHz)              | Ka                      | Ka              | Ka               | Ka           |
|                                      | 500                     | 500             | 500              | 500          |
|                                      | Q                       | Q               | Q                | Q            |
|                                      | 1000                    | 1000            | 1000             | 1000         |
| Roll off factor                      | W                       | W               | W                | W            |
|                                      | 1000                    | 1000            | 1000             | 1000         |
| Roll off factor                      | 0.25                    | 0.25            | 0.25             | 0.25         |
| Mod/Cod                              | Extended CCSDS standard |                 |                  |              |

B. Clear sky link budget analysis

The link budget formulae are found in Appendix [1] were used to derive the clear sky link budget tables for all sites as will be shown in the results subsection at each of Ka, Q and W bands.

C. Channel model

Precipitation loss evaluation was the first phase of the total channel degradation evaluation as mentioned previously. Attenuation due precipitation was provided by the ITU-R P.618 [14]. The unconditional probability distribution and the complementary cumulative distribution functions of rain attenuation as a function of elevation angle were evaluated as follows as provided by equations 1 and 2 respectively.

$$P_A(A) = \frac{1}{\sqrt{2\pi} S_A} e^{-\frac{\ln^2(\frac{A}{A_m})}{2S_A^2}} \tag{1}$$

$$P(A > A_m) = \frac{1}{2} \operatorname{erfc}\left(\frac{\ln(\frac{A}{A_m})}{\sqrt{2} S_A}\right) \tag{2}$$

$A_m$  is the median value of rain attenuation and  $S_m$  is the standard deviation of  $\ln A$ . Rainy and non- rain period were taken into account.

Precipitation introduces an increase in the gateway’s system noise temperature this increase was evaluated by equation 3 as in [18]

$$T_{\text{total}} = 10 \log (T_{\text{system clear sky}} + \alpha 275 (1 - 10^{-\frac{\text{loss precipitation}}{10}})) \text{K} \tag{3}$$

Total channel degradation was evaluated based on the model provided by ITU-R P.1853 [14] for water vapor, clouds and oxygen attenuation, and ITU-R P.618-12 [14] for scintillation. Then the total channel degradation from [1] was evaluated as in equation 4 which involved the contribution of the degradation due to the increase in antenna noise temperature caused by precipitation.

$$A_{\text{Satellite Channel}} = A_{\text{Water vapour}} + A_{\text{Oxygen}} + A_{\text{rain}} + A_{\text{Clouds}} + A_{\text{Scintillation}} + T_{\text{Faded}} \text{ dB} \tag{4}$$

The total channel degradation complementary cumulative distribution function at Redu, Harwell, Weilham and Matera at Ka, Q and W bands was generated and verified by the complementary cumulative distribution in [14]

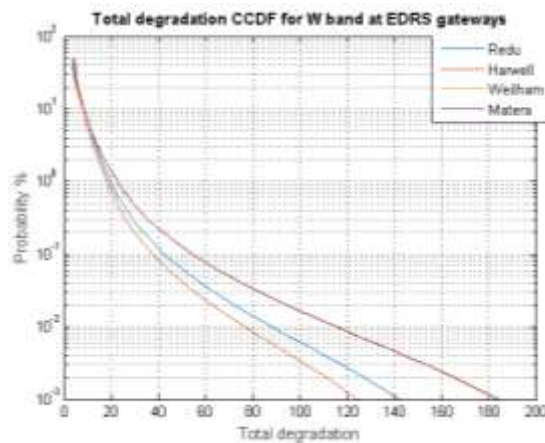


Fig.3. Total channel degradation CCDF at W band for all four primary gateways.

D. Average link capacity

First of all the clear sky signal to noise ratio was evaluated

$$\frac{S}{N} \text{ Clear sky} = P_T + G_T - L_T - FSL - A_{gas} + G_{RX} - 10 \log(T_{RX}) - 10 \log(B) + k \text{ dB} \quad (5)$$

Where  $P_T$  the transmission power (dB),  $G_T$  is the transmitter antenna gain (dB),  $L_T$  is transmitter loss (dB),  $FSL$  free space path loss (dB),  $A_{gas}$  is gaseous absorption of water vapour and oxygen (dB),  $G_{RX}$  is the receiver antenna gain (dB),  $T_{RX}$  is system noise temperature (K),  $B$  is the channel bandwidth (Hz),  $k$  is the Boltzmann constant which is equal to 228.6 dB.

Total channel degradation evaluated was then added to the clear sky signal to noise ratio

$$\frac{S}{N} \text{ Faded} = \frac{S}{N} \text{ Clear sky} - A_{\text{Satellite Channel}} \text{ dB} \quad (6)$$

Referring to the extended CCSDS modulation and coding schemes list the minimum required signal to noise ratio of each scheme which was further degraded as mentioned in [1]. In return the threshold signal to noise ratio of each modulation and coding increased

$$\frac{S}{N} \text{ Threshold} = \frac{S}{N} \text{ Minimum} + \text{Additional Degradation} \text{ dB} \quad (7)$$

The transmitting satellite power was backed off as a function of the modulation and coding scheme used to avoid the amplifier from operating in the nonlinear region. The back off values were provided by [1]

$$\frac{S}{N} \text{ Received} = \frac{S}{N} \text{ Faded} - \text{OBO} \text{ dB} \quad (8)$$

Maximum tolerable attenuation for each modulation and coding can be defined as threshold attenuation and expressed as shown in the equation below

$$A_{Th} = \frac{S}{N} \text{ Clear Sky} - \frac{S}{N} \text{ Threshold} \text{ dB} \quad (9)$$

Probability of each modulation and coding scheme is hence dependent on the total channel degradation and the threshold allowable attenuation of each scheme.

$$P(\text{Mod/Cod}) = P\left(\frac{S}{N} \text{ Received} \geq \frac{S}{N} \text{ Threshold}\right) = P(A_{\text{Satellite Channel}} \leq A_{Th}) \quad (10)$$

Recall now the total degradation complementary cumulative distribution function evaluated for two different cases. Case one was for the highest order modulation and coding scheme which required the highest received signal to noise ratio and hence smallest allowable degradation was evaluated by

$$P(\text{Mod/Cod Highest order}) = P(A_{\text{Satellite Channel}} \leq A_{\text{Th Lowest}}) = 1 - P(A_{\text{Satellite Channel}} > A_{\text{Th Highest}}) \quad (11)$$

The second case for all other modulation and coding schemes which was evaluated by

$$P(\text{Mod/Cod (i)}) = P(A_{\text{Th(i-1)}} < A_{\text{Satellite Channel}} \leq A_{\text{Th (i)}}) = P(A_{\text{Satellite Channel}} > A_{\text{Th(i-1)}}) - P(A_{\text{Satellite Channel}} > A_{\text{Th(i)}}) = P(A_{\text{Satellite Channel}} \leq A_{\text{Th(i)}}) - P(A_{\text{Satellite Channel}} \leq A_{\text{Th(i-1)}}) \quad (12)$$

The Average capacity was evaluated by equation 13 for the gateway at Matera, Italy and then compared to the average capacity evaluated in [1] for formulae verification

$$C = \sum_{i=0}^n P(i) \times \eta(i) \times R_s \text{ bps} \quad (13)$$

Where P (i) is the probability of each modulation and coding scheme. ,  $\eta$  is the modulation and coding scheme spectral efficiency and  $R_s$  is the symbol rate.

Link availability was evaluated by equation 14 and verified by comparing to the availability evaluated in [1] for the gateway in Matera, Italy. Using the same formulae availability of each modulation and coding scheme was evaluated using the modulation and coding scheme threshold attenuation derived in equation 9

$$\text{Availability} = P(A_{\text{Satellite Channel}} > A_{\text{Th Highest}}) = 1 - P(A_{\text{Satellite Channel}} \leq A_{\text{Th Highest}}) \quad (14)$$

### E. Site diversity model

Initially, single site total degradation and rain attenuation complementary cumulative distribution functions were evaluated for the all primary and redundant gateways using the previously explained methodology. For each primary gateway there were three redundant gateways at separation distances of 20 Km, 50 Km and 80 Km. All redundant gateways had identical parameters to the primary gateways mentioned previously given that they operated at the same frequency band. The site diversity model was verified by results comparison to [14, 19, 20, and 21].

#### 1) Signal combining

Primary and redundant gateways were terrestrially connected to combine the received signal at each terminal using any of the combining techniques. It was assumed that the terrestrial connection was perfectly synchronized for channel information exchange and channel detection was assumed to be ideal, hence downlink channel gain provided by [34] was modelled by

$$h_t = |h_t| e^{j\theta} \quad (15)$$

$$|h_t| = 10^{\frac{-A_t}{20}} \quad (16)$$

Where A was the single link total degradation evaluated in equation 4.

Site diversity was modelled for selective combining (SC), equal gain combining (EGC) and maximum gain combining (MGC). The combined received signal to noise ratio from both gateways was provided by [19] for equal and maximum gain combining and [20] for selective combining.

$$snr_{DIVERSITY} \begin{cases} \frac{snr_{RX}}{SD} = Max ( |h_1|^2, |h_2|^2 ) snr_{clear\ sky} \\ \frac{snr_{RX}}{EGC} = \frac{1}{2} ( |h_1| + |h_2|^2 )^2 snr_{clear\ sky} \\ \frac{snr_{RX}}{MGC} = ( |h_1|^2 + |h_2|^2 ) snr_{clear\ sky} \end{cases}$$

$$SNR_{Diversity} = 10 \log ( snr_{Diversity} ) \quad (17)$$

2) *Linkoutage probability*

Single link outage probability is the probability that the signal to noise ratio received falls below the predefined threshold signal to noise ratio, it was evaluated by solving equation 18 using the total channel degradation complementary cumulative distribution function derived in equation 4

$$P_{outage} = Pr [ SNR_{RX} \leq SNR_{Th} ] = Pr [ A_{Th} \geq SNR_{clear\ sky} - SNR_{Th} ]$$

$$= \int_{SNR_{clear\ sky} - SNR_{Th}}^{\infty} P_{Total\ degradation} (x) dx \quad (18)$$

3) *Sitediversity outage probability*

Let  $P_{Outage} (A1)$  and  $P_{Outage} (A2)$  be the single link outage probabilities of the primary and the redundant gateways hence diversity link outage  $P_{Outage} (A1, A2)$  can be expressed using Bayes theorem as shown in equation 19 where  $P (A2|A1)$  is defined as the outage probability of the redundant link given that the primary link is already in outage.

$$P_{Outage} (A1, A2) = P_{Outage} (A2) * P_{outage} (A1|A2) = P (A1 \geq a1, A2 \geq a2) \quad (19)$$

Detailed methodology of the diversity link outage due to rain attenuation was provided by [14] and used by references [19] and [20]. Equation 20 was provided by [14] which transformed the general expression derived in equation 19 to the product of  $P_r$  which was the probability of rain at both sites and  $P_a$  which was the conditional probability that rain attenuation exceeds the thresholds  $a1$  and  $a2$  at each gateway.

$$P (A1 \geq a1, A2 \geq a2) = 100 \times Pr \% \times Pa \% \quad (20)$$

$P_r$  and  $P_a$  are complementary bivariate normal distributions evaluated by equations 21 and 22 respectively

$$P_r = \frac{1}{2\pi\sqrt{1-\rho_r^2}} \int_{R1}^{\infty} \int_{R2}^{\infty} e^{-\frac{r1^2 - 2\rho_r r1r2 + r2^2}{2(1-\rho_r^2)}} dr1dr2 \quad (21)$$

$$\rho_r = 0.7e^{-\frac{D}{30}} + 0.3e^{-\left(\frac{D}{700}\right)^2}$$

$$P_a = \frac{1}{2\pi\sqrt{1-\rho_a^2}} \int_{\ln a1 - \ln A1}^{\infty} \int_{\ln a2 - \ln A2}^{\infty} e^{-\frac{a1^2 - 2\rho_a a1a2 + a2^2}{2(1-\rho_a^2)}} da1da2 \quad (22)$$

$$\rho_a = 0.94e^{-\frac{D}{30}} + 0.06e^{-\left(\frac{D}{500}\right)^2}$$

Where D is the separation distance between two sites (Km) , R1 and R2 are thresholds for sites 1 and 2, evaluated by equation 23 ,  $\rho_r$  measure of rain probability correlation between the two sites ,  $\rho_a$  measure of rain attenuation correlation between the two sites , Probability of rain at each site in equation 21 was evaluated referring to the methodology provided by [22] ITU-recommendations P.837 , Parameter  $mln_{A1}$ ,  $mln_{A2}$ ,  $\sigma ln_{A1}$  and  $\sigma ln_{A2}$  were determined by fitting each single site rain attenuation and its probability of occurrence.

$$R_k = Q^{-1}\left(\frac{P_k^{rain}}{100}\right) \quad (23)$$

Using this methodology joint rain attenuation is expressed by equation 24 as in [20] where  $\rho$  is the spatial correlation coefficient between the two sites.

$$f_{A_1, A_2}(A_1, A_2) = \frac{1}{2\pi\sigma_1\sigma_2\sqrt{1-\rho^2}} \exp\left(-\frac{1}{1-\rho^2} [u_1^2 - 2\rho u_1 u_2 + u_2^2]\right) \quad (24)$$

$$u_i = \frac{\ln A_i - m_i}{\sigma_i}, i=1, 2$$

$$\rho = 0.94 \exp\left(-\frac{D}{30}\right) + 0.06 \exp\left(-\left(\frac{D}{500}\right)^2\right)$$

The final expression of the diversity link outage probability as in [19,20] and expressed by equation 24 and presented graphically in figure 13 by evaluating the area above the curve when the received and combined signal to noise ratio is equal to the threshold value where  $P_{Ar1,Ar2}$  is the joint lognormal rain attenuation probability density function in 24.

$$P_{out} = \Pr [A_{Instantaneous} \geq SNR_{clear Sky} - SNR_{Th}] \int_{A2}^{\infty} \int_{A1,2}^{\infty} P_{Ar1,Ar2}(x, y) dx dy \quad (25)$$

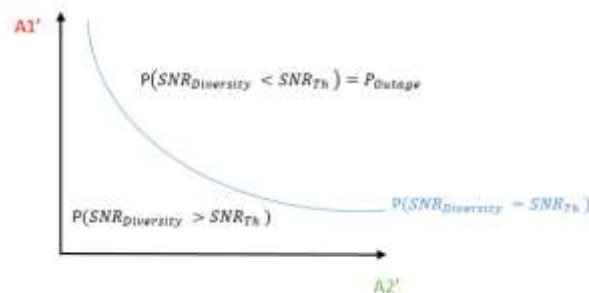


Fig.4. Graphical solution of the diversity link outage probability.

Equations set 17 was originally derived from equations set 26 as in [19, 20], A2 and A1, 2 were solved using equations sets 27 and 28 derived from [19, 20]

$$c(A1, A2) \left\{ \begin{array}{l} \text{Selevtive combinging (SC)} = \\ \quad (\max(10^{-\frac{A_1}{10}}, 10^{-\frac{A_2}{10}})) + \\ \text{SNR}_{clear\ sky} - \text{SNR}_{Th} - K, K = 0dB \\ \\ \text{Equal gain combining(EGC)} = \\ \quad 20\log_{10}(\max(10^{-\frac{A_1}{20}} + 10^{-\frac{A_2}{20}})) + \\ \text{SNR}_{clear\ sky} - \text{SNR}_{Th} - K, K = 3dB \\ \\ \text{Maximaum gain combining (MGC)} = \\ \quad 10\log_{10}(10^{-\frac{A_1}{10}} + 10^{-\frac{A_2}{10}}) + \\ \text{SNR}_{clear\ sky} - \text{SNR}_{Th} - K, K = 0d \end{array} \right. \quad (26)$$

$$c(\infty, A2) \left\{ \begin{array}{l} A2 = A_{Th}, SC \\ A2 = A_{Th} - 3, EGC \\ A2 = A_{Th}, MGC \end{array} \right. \quad (27)$$

Where A2 was the solution of equations set 26 C ( $\infty, A_{2\infty}$ ) = 0 when the first link is already in outage at a very high attenuation value. Where A2 was the solution of equations - set 27 C ( $\infty, A_{2\infty}$ ) =0 when the first link is already in outage at a very high attenuation value.

$$A_{2\infty} \begin{cases} 0 & A_{2\infty} < 0 \\ A_{2\infty} & A_{2\infty} > 0 \end{cases}$$

$$c(A12, A2) \left\{ \begin{array}{l} A12 = A_{Th}, SC \\ A12 = -20\log_{10}(\max(10^{-\frac{A_{Th}+A_2}{20}} - 10^{-\frac{A_2}{20}})), EGC \\ A12 = -10\log_{10}(10^{-\frac{A_{Th}}{10}} - 10^{-\frac{A_2}{10}}), MGC \end{array} \right. \quad (28)$$

The model proposed by ITU-Recommendations P.618-12 [14] evaluated diversity link outage probability due to rain attenuation only as mentioned before and hence spatial rain correlation was included as provided by equation 21 and clouds spatial correlation and any other factor needed for diversity link outage due to total degradation was excluded.

Equation 24 is solved when Ar1 and Ar2 are the rain attenuations and hence equations sets 26, 27 and 28 were solved with A2 and A1, 2 being the total channel degradation and then A2 and A1, 2 were mapped to the equivalent rain attenuation for the same exceedance probability using the rain attenuation and the total channel degradation complementary cumulative distribution functions previously. Equation 25 was solved numerically using all the previously evaluated parameters. Diversity gain was evaluated by equation 29 referring to [19, 23] as a function of time percentage. At last, the system's average capacity and availability were evaluated for the diversity link as will be shown in the next section.

$$\text{Diversity gain} = \text{SNR}_{Diversity\ Link} - \text{SNR}_{Single\ Link} \quad (29)$$

IV. RESULTS

Total link degradation distribution function was the key to solve for the gateway average capacity and hence the probability mass function of the extended CCSDS modulation and coding schemes was generated as shown in figures for all gateways each evaluated at Ka, Q and W bands. All figures were logarithmically scaled, and the x axis represented the modulation scheme index as arranged in [1] while the y-axis represented the probability of using the equivalent modulation and coding scheme in percentage. Figure 5 shows the probability mass function (PMF) of each modulation and coding scheme for the gateway in Matera, Italy at W band.

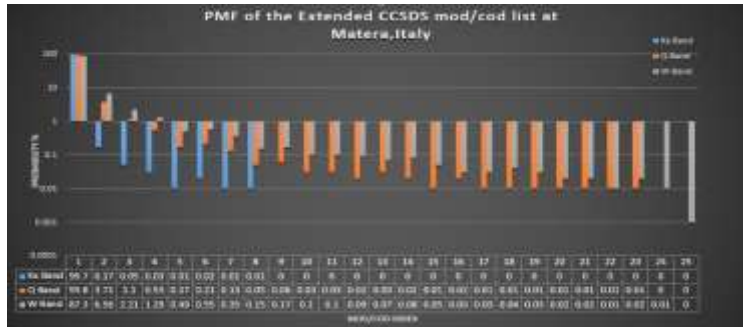


Fig. 5. Extended CCSDS mod/cod list probability mass function at Matera, Italy at Ka, Q and W bands

The probability mass functions evaluated were used to evaluate the single link capacity and availability analysis at each frequency band for each of the four primary gateways. Table 2 displays single link maximum, average capacity in gigabits per second (Gbps) and availability in percentage (%) for each of the four gateways at W band.

TABLE II. MAXIMUM & AVERAGE SINGLE LINK CAPACITY

| Frequency Band | Gateway | Maximum Capacity Gbps | Average Capacity Gbps | Availability % |
|----------------|---------|-----------------------|-----------------------|----------------|
| Q Band         | Redu    | 6.8                   | 6.66                  | 99.98          |
|                | Harwell | 6.8                   | 6.69                  | 99.98          |
|                | Weilham | 6.8                   | 6.65                  | 99.97          |
|                | Matera  | 6.8                   | 6.65                  | 99.97          |
| W Band         | Redu    | 6.8                   | 0.96                  | 99.96          |
|                | Harwell | 6.8                   | 0.96                  | 99.97          |
|                | Weilham | 6.8                   | 0.688                 | 99.94          |
|                | Matera  | 6.8                   | 0.288                 | 99.94          |

Figures 6 shows the received and combined signal to noise ratio of nine site diversity scenarios where selective combining (SC), equal gain combining (EGC) and maximum gain combining (MGC) were employed at three gateway separation distances of 20Km ,50 Km and 80 Km for each of the gateway in Italy. The time percentage was logarithmically plotted for the equivalent received and combined signal to noise ratio for each of the combining techniques. All diversity scenarios were plotted in comparison with the single link.

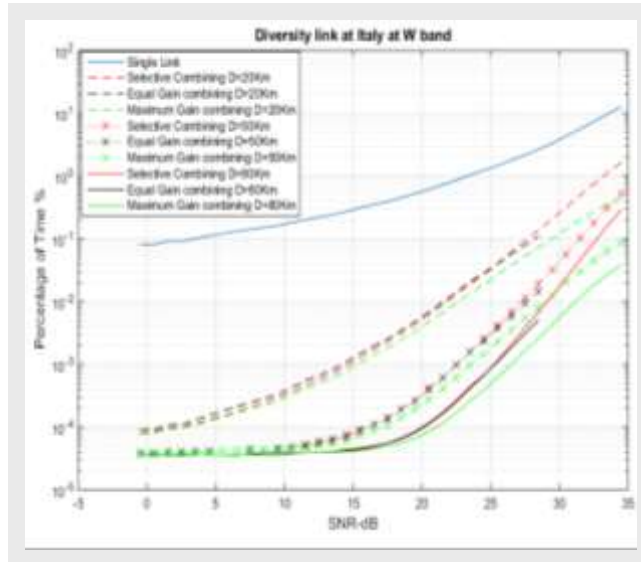


Fig. 6. Received and combined signal to noise ratio at gateway in Italy

Table 3 shows the evaluated diversity link availability and average capacity when each of the combining techniques was applied to each of the four primary gateways at Q and W bands with gateways separation distance of 80 Km.

TABLE III. LINK AVAILABILITY & AVERAGE CAPACITY IN SITE DIVERSITY SCENARIO

| Gateway | Freq | Selective Combining |                       | Equal Gain Combining |                       | Maximum Gain Combining |                       |
|---------|------|---------------------|-----------------------|----------------------|-----------------------|------------------------|-----------------------|
|         |      | Link Availability % | Average capacity Gbps | Link availability %  | Average capacity Gbps | Link availability %    | Average capacity Gbps |
|         |      |                     |                       |                      |                       |                        |                       |
| Belgium | Q    | 99.999              | 6.7221                | 99.999               | 6.7225                | 99.999                 | 6.7313                |
|         | W    | 99.994              | 6.7221                | 99.999               | 6.7221                | 99.999                 | 6.7802                |
| England | Q    | 99.999              | 6.7386                | 99.999               | 6.7885                | 99.999                 | 6.7992                |
|         | W    | 99.994              | 6.7281                | 99.999               | 6.7881                | 99.999                 | 6.7991                |
| Germany | Q    | 99.998              | 6.7314                | 99.999               | 6.7335                | 99.999                 | 6.7382                |
|         | W    | 99.997              | 6.3281                | 99.999               | 6.4885                | 99.999                 | 6.7802                |
| Italy   | Q    | 99.998              | 6.7221                | 99.999               | 6.7228                | 99.999                 | 6.7331                |
|         | W    | 99.996              | 6.3280                | 99.999               | 6.4883                | 99.999                 | 6.7802                |

## V. CONCLUSION

Migration to Ka, Q and W bands was one proposed solution to achieve high capacity earth observation link and this was applied by establishing a data relay link that collects data from low earth orbit satellites and retransmit it to the gateways at much higher capacities. Propagation channel at Ka, Q and W bands is very challenging especially at Q and W bands where site diversity was the only solution to establish a high availability feeder down link. Channel models were derived for each frequency band and formulae to predict the average capacity when variable code and modulation fade mitigation technique was employed. Then four links were designed at Ka band for the four European earth observation programmes gateways where variable code and modulation fade mitigation technique was employed to successfully achieve a data rate of 3.39 Gbps and a link availability of 99.99% for all links. At Q and W bands the designed links employed site diversity with selective, equal gain and maximum gain combining techniques which were modelled and evaluated for three diversity scenarios with different gateways separation distances. The designed Q and W band links were at gateways separation distance of 80 Km, they achieved availability of 99.99% for all combining techniques and had a minimum average capacity of 6.7 Gbps and 6.4 Gbps respectively.

## REFERENCES

- [1] Z.K, C.K, A.D, N.J, Capacity analysis of high throughput satellite links for earth observation missions, International Journal of Satellite Communications and Networking, pages429-449, Vol.33, No.5, 2015.
- [2] Meteosat Third Generation (MTG) will see the launch of six new satellites from 2020, EU METSAT, available at <http://www.eumetsat.int/website/home/Satellites/FutureSatellites/MeteosatThirdGeneration/index.html> viewed February 2016
- [3] Environmental Mapping and Analysis Program, DLR 2014, available at: <http://www.enmap.org/>, viewed on February 2016
- [4] MeteosatThirdGeneration, eoPortalDirectory, available at <https://directory.eoportal.org/web/eoportal/satellite-missions/m/meteosat-third-generation>
- [5] European space agency operations, ESA, available at: [http://www.esa.int/Our\\_Activities/Operations/Earth\\_observation\\_missions](http://www.esa.int/Our_Activities/Operations/Earth_observation_missions).
- [6] Earth Observation Satellites, Copernicus, available at: <http://www.copernicus.eu/main/satellites> Viewed on April 2016
- [7] Sentinel-1 mission overview. ESA .2014, Available at: <https://sentinel.esa.int/web/sentinel/missions/sentinel-1/overview>, viewed on April 2016
- [8] European data relay system, Infrastructure, available at: [http://www.esa.int/Our\\_Activities/Telecommunications\\_Integrated\\_Applications/EDRS/Infrastructure](http://www.esa.int/Our_Activities/Telecommunications_Integrated_Applications/EDRS/Infrastructure), viewed on: 22nd June 2016.
- [9] ViaSat-1 is transforming the Economics and Quality of Service for Satellite Broadband, ViaSat available at: <https://www.viasat.com/viasat-1-launch>, viewed on April 2016.
- [10] C. S, M. L, T. R, E. C, M. R , Transponders research analysis for the development of telecommunication Payloads in Q/V bands, 2009 IEEE Aerospace conference, pages1-11, March 2009
- [11] C.R, C.C, L.L, M.L, R.N, A.M, The challenge of using the W band in satellite communication, International Journal of Satellite Communications and Networking, Vol.32, No.3, August 2013
- [12] D.G, E.L, J.P,R.M,A High-Throughput Satellite System for serving whole Europe with Fast Internet Service, Employing Optical Feeder Links, Broadband Coverage in Germany. 9th ITG Symposium. Proceedings, pages1-7, Berlin, Germany, April 2015.

- [13] O.V, G.V, J.L, E.A, J.R, M.B, Next generation high throughput Satellite system, 2012 IEEE First AESS European Conference on Satellite Telecommunications (ESTEL), pages1-7, Rome,Italy, 5 October 2012.
- [14] Propagation data and prediction methods required for the design of Earth-space telecommunication Systems-R P.618, 2012
- [15] ] C.R, C.C, L.L, M.L, R.N, A.M, the challenge of using the W band in satellite communication, International Journal of Satellite Communications and Networking, Vol.32, No.3, August 2013.
- [16] European data relay system, Infrastructure, available at:[http://www.esa.int/Our\\_Activities/Telecommunications\\_Integrated\\_Applications/EDRS/Infrastructure](http://www.esa.int/Our_Activities/Telecommunications_Integrated_Applications/EDRS/Infrastructure), viewed on: 22nd June 2016.
- [17] Sputnik and the dawn of the space age, NASA, available at: <http://history.nasa.gov/sputnik/>, viewed on April 2016
- [18] Evans, Barry, Satellite Communications systems, 4th Edition, The Institution of Engineering and Technology; 4 editions, November 15, 2011.
- [19] P-D. A, B.S, A.D.P, B.O, Gateway Diversity strategies in Q/V band feeder links, 17th Ka and Broadband Communications Conference, pages 1384-1387, Palermo, Italy, 3-5 October 2011
- [20] A.G, B.S, P.A B. O, Gateway Switching in Q/V Band Satellite feeder links, IEEE Communications surveys of the electronic magazine, Vol.17, No.7, pages 1384-1387, 23 July 2013
- [21] ITU-R Recommendation P.1815-0, "Differential rain attenuation," Geneva, Switzerland, 2007.
- [22] Characteristics of prediction for propagation modelling, ITU-R P.837, 2012.
- [23] R.V, Performance Evaluation of Equal Gain Diversity Systems In Fading Channels, Master of science Thesis, Virginia Polytechnic Institute and State University, 2003 available at: [https://theses.lib.vt.edu/available/etd-12282003-180042/unrestricted/Ramanathan\\_V\\_ETD.pdf](https://theses.lib.vt.edu/available/etd-12282003-180042/unrestricted/Ramanathan_V_ETD.pdf), viewed on August 2016

APPENDIX – LINK BUDGET FORMULAEAS

**Constants**

Boltzmann constant,  $k = -228.6$  dBW/K/Hz

Radius of the Earth = 6378 km

Free Space Path Loss (FSPL)

$$\text{elevation angle } (el) = \tan^{-1} \left( \frac{\cos(\beta) - \sigma}{\sin(\beta)} \right) \text{ deg}$$

$$\text{azimuth angle } (az) = \tan^{-1} \left( \frac{\tan(\phi_s)}{\sin(\theta_s)} \right) + 180^\circ \text{ deg from true North}$$

$$\text{range } (d) = 35,786 \sqrt{(1 + 0.4199(1 - \cos(\beta)))} \text{ km}$$

Where:-

$$\beta = \cos^{-1}(\cos(\theta_s) \cos(\phi_s))$$

$$\phi_s = (\phi_e - \phi_s)$$

$$\sigma = \frac{r}{r+h}$$

$\phi_e$  = longitude of earth station (positive East)

$\theta_s$  = latitude of earth station (positive North)

$\phi_s$  = longitude of satellite (positive East)

$r$  = radius of the Earth (6,378 km)

$h$  = height of satellite above equator ( 35,786 km)

$$\text{FSPL} = 20 \log_{10} \left( \frac{4 \pi \text{ Range}_m}{\lambda} \right)$$

**Figure of Merit: G/T**

$$G/T = G_{ant_{dB}} - 10 \log_{10}(T_e) \text{ dB/K}$$

**Antenna Gain**

$$G = \frac{4 \pi A_e}{\lambda^2}$$

Where  $A_e$  is the effective area given by:-

$A_e$  is the effective aperture area of the antenna given by  $A_e = \eta A$  with  $\eta$  being the ante efficiency (normally between 0.4 and 0.80, can also be expressed in %) and with  $A$  bei physical aperture area.

**Noise Temperature and Noise Figure relationships**

$$NF = 10 \log_{10} \left( 1 + \frac{T}{290} \right) \text{ dB}$$

$$T = 290 (10^{NF/10} - 1) \text{ K}$$

**Increase in System Noise Temperature due to precipitation**

$$T_{inc} = \alpha \times 275 \left( 1 - 10^{(-Loss_{prec}/10)} \right) \text{ K}$$

(referred to the LNA input reference plane)

**System Noise Temperature**

$$T_s = \alpha T_A + (1 - \alpha) T_F + T_R \text{ K (clear sky conditions)}$$

(referred to the LNA input reference plane)

Where:-

$T_A$  = Antenna noise temperature (K)

$T_F$  = Feeder noise temperature (K), normally 290 K

$T_R$  = Receiver noise temperature (K)

$$\alpha = 10^{(-L/10)}$$

With feeder loss being  $L$  (dB)

$$\text{Antenna beamwidth (approximately)} \theta_{3dB} = \frac{21}{f_{GHz} \times d_m} \text{ deg}$$

**Symbol rate**

$$\text{Symbol Rate} = \frac{\text{Information bit rate}}{m \times r}$$

**Occupied bandwidth**

$$\text{Occupied bandwidth } (B) = \text{Symbol Rate} \times (1 + \alpha)$$

**Determining the required C/N from the required Eb/No and vice versa**

$$C/N = \frac{E_b}{N_o} - 10 \log_{10}(1 + \alpha) + 10 \log_{10}(m) + 10 \log_{10}(r) \text{ dB}$$

$$\frac{E_b}{N_o} = C/N + 10 \log_{10}(1 + \alpha) - 10 \log_{10}(m) - 10 \log_{10}(r) \text{ dB}$$

Where:

$\alpha$  = the filter roll-off factor ( 0 to 1)

$r$  = the overall FEC rate e.g. for DVB concatenated RS and Viterbi  $\frac{3}{4}$

$$r = 3/4 \times 188 / 204 = 6911$$

$m = \log_2(M)$  where  $M$  is the number of phase states

|        | M  | m |
|--------|----|---|
| BPSK   | 2  | 1 |
| QPSK   | 4  | 2 |
| 8PSK   | 8  | 3 |
| 16APSK | 16 | 4 |
| 32APSK | 32 | 5 |

**C/N<sub>0</sub>**

$$\frac{C}{N_o} \text{ (dB)} = \text{EIRP} \text{ (dBW)} - \text{losses} \text{ (dB)} + \frac{G}{T} \text{ (dB)} + 228.6 \text{ dB/Hz}$$

Also:-

$$C/N_o = C/N + 10 \log_{10}(B) \text{ dB/Hz}$$

And:-

$$C/N = C/N_o - 10 \log_{10}(B) \text{ dB}$$

$B$  is the occupied bandwidth in Hz.

